INVESTIGATION OF CoNiCr THIN FILMS DEPOSITED ON [100] AND [110] Cr SINGLE CRYSTALS

B.Y.Wong
Dept. of Metallurgical Engineering
and Materials Science
Carnegie Mellon University
Pittsburgh, PA15213

D. E. Laughlin
Dept. of Metallurgical Engineering
and Materials Science
Carnegie Mellon University
Pittsburgh, PA15213

D.N. Lambeth
Dept. of Electrical and
Computer Engineering
Carnegie Mellon University
Pittsburgh, PA15213

***Abstract*——$Co_{62.5}Ni_{30}Cr_{7.5}$ thin films were sputtered onto [100] and [110] Cr single crystals as well as polycrystalline Cr TEM foils. VSM measurements have revealed the existence of an anisotropy in the in-plane coercivity. This stems from the development of a crystallographic texture in the plane of the film. TEM investigations have found the presence of crystallographic variants in the direction of the hcp c-axis in the CoNiCr films deposited on (100) and (110) Cr surfaces. Lorentz microscopy studies have found relatively straight domain walls which lie parallel to the specific crystallographic directions. The direction of magnetization within each domain is along the c-axis.**

I. Introduction

The enhancement of in-plane coercivity of Co-based alloy thin films by the addition of a Cr-underlayer is a well known phenomenon[1] and it is often used in the preparation of thin film magnetic recording media. Previous structural investigations[2-4] have indicated that the underlayer exerts a great influence on the crystallographic structure and the microstructure of the magnetic layer. X-ray and Transmission Electron Microscopy (TEM) studies have shown the existence of orientation relationships (O.R.) between the Cr-underlayer and the magnetic layer, thus giving rise to a preferred in-plane texture of the hcp c-axis. However, such a texture is fibrous in nature and the orientation of the c-axis is random in the plane of the film. A fibrous texture denotes that all the grains in the film have the same crystallographic zone axis parallel to the normal of the film but there is no preferred alignment of crystal axis in the plane. The present work has achieved in acquiring an in-plane crystallographic texture by depositing CoNiCr thin films on [100] and [110] Cr single crystals and also large Cr grains. This paper reports the effect of such in-plane crystallographic texture on the magnetic properties and the magnetic domain structure of CoNiCr films.

II. Sample Preparation and Characterization

Two types of chromium substrate were prepared for deposition. First, single crystal discs of chromium with [100] and [110] orientation were mechanically polished with carbide papers and alumina wheels to obtain a flat surface. The final polishing was carried out with 0.05μm alumina. The discs are about 14mm in diameter and 2mm thick. The second type of specimens were polycrystalline 3mm diameter TEM Cr-foils prepared by the standard electrochemical jet polishing technique. The Cr grain size in these foils is in the mm range. The polishing solution consisted of 10% percholic acid and 90% methanol by volume and polishing was carried out at -20°C at a potential of 15V. Deposition of CoNiCr on both types of Cr substrates was carried out in a LH Z-400 sputtering system. The base pressure in the deposition chamber was $4x10^{-7}$Torr. The Argon sputtering gas pressure was 10mTorr with a rf forward power of 100W over a 3inch target. The specimens were first sputter etched at room temperature for 20min before deposition of CoNiCr to remove the oxide layer and any hydrocarbons that were present. The magnetic properties were measured by a vibrating sample magnetometer. The crystallographic structure of the films deposited on the single crystals were studied by X-ray diffraction with Cu-Kα radiation and the foil specimens were studied by TEM. The composition of the sputtering target was Co62.5-Ni30-Cr7.5(at%) and the thickness of the deposited layer was 400Å for all the specimens.

III. Results and Discussion

The X-ray diffraction spectra for CoNiCr films deposited on [100] and [110] Cr single crystals are shown in Figure 1. In the [100] Cr spectrum, both fcc CoNiCr (200) reflection and hcp $(11\bar{2}0)$ diffraction peaks are present. The $(11\bar{2}0)$ reflection is the result of the epitaxial growth between the CoNiCr grains and the (100) Cr surface and this indicates that the surface oxide layer has been removed through sputter-etching. The O.R. is that of Pitsch-Schrader, (0001)hcp//(011)bcc, $[11\bar{2}0]$hcp//[100]bcc. The (200) fcc plane does not match well with the (100) Cr surface through any existing bcc:fcc O.R. The only possible O.R. which agrees with the observation is that of Bain, which has never been observed in the Co/Cr systems. In the [110] Cr spectrum, only the hcp CoNiCr $(10\bar{1}1)$ reflection is observed. This corresponds to the Potter O.R., $(10\bar{1}1)//(1\bar{1}0)$, $[11\bar{2}0]//[111]$, between the CoNiCr film and the underlying single crystal. The broadness of

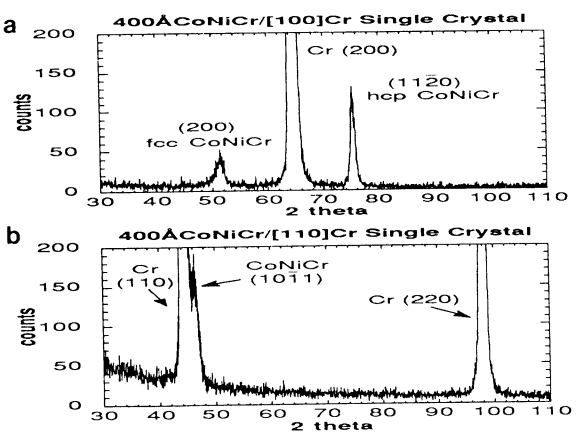

Figure 1. X-ray diffraction spectra of CoNiCr films deposited on (a) [100] and (b) [110] Cr single crystals.

Presented at IEEE Intermag, June, 1991. This research was supported by the DOE under Grant no. DE-FG02-90ER45423. We also acknowledge the use of facilities which are supported by the NSF under Grant no. ECD-8907068. The government has certain rights to this material.

the Cr peaks is probably due to the defects introduced by the lapping process. TEM diffraction studies of CoNiCr films deposited on Cr foils have revealed the existence of different crystallographic variants for both the O.R. stated above. Figure 2a shows the diffraction pattern of CoNiCr film deposited on a (100) Cr grain surface. It is seen that the hcp c-axis lies parallel to either the [110] or the [1$\bar{1}$0] directions. Streaks, which came about due to planar defects, can be observed along the [0002] direction. In the case of a (110) Cr surface (Figure 2b), the projection of the c-axis is parallel to either the [$\bar{1}$12] or the [$\bar{1}1\bar{2}$] directions of Cr. Diffuse elongated intensity can also be **observed** along these directions.

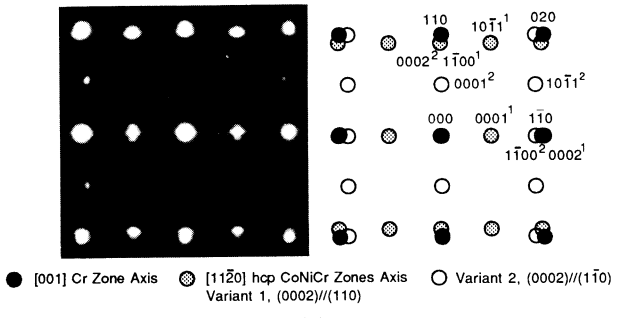

(a)

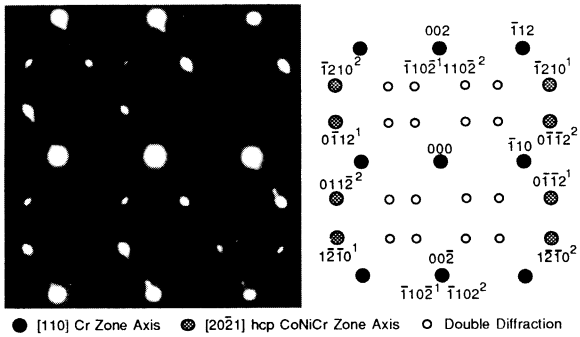

(b)

Figure 2. SAD pattern for CoNiCr films deposited on (a) (001) and, (b) (110) Cr grain surfaces. The O.R. is that of Pitsch-Schrader in (a) and Potter in (b).

The coercivity and the switching squareness measured along various crystallographic directions of the Cr single crystals are listed in table 1. The difference in coercivity is due to the presence of a in-plane crystallographic texture. Figure 3 shows the VSM loops measured along the [$\bar{1}1\bar{1}$] and [$\bar{1}$11] of the (110) single crystal. The sloping of the loop after saturation is due to the antiferromagnetic nature of the chromium substrates. Since the coercivity is much smaller than the anisotropy field, magnetization reversal is most likely carried out by domain wall motion. The coercivities of CoNiCr films deposited on the single crystals are smaller than those measured in polycrystalline specimens with strong fibrous texture[4]. This may be the consequence of the preferential grain alignment in the CoNiCr film, thus enhancing the exchange coupling between grains[5,6]. As a result, domain wall motion is made easier. In the case of the (100) single crystal, the presence of the fcc CoNiCr may also have contributed to the decrease in coercivity. The S* values shows that the hysteresis loops are less square along either [0002] or its projection.

Table.1
The in-plane coercivity and switching squareness along various crystallographic directions of the Cr single crystals.

Crystal	Direction	H_c(Oe)	S*
(001)	[100]	475	0.46
	[110]	315	0.12
(110)	[$\bar{1}1\bar{1}$]	233	0.24
	[$\bar{1}$11]	485	0.91
	[$\bar{1}1\bar{3}$]	535	0.61

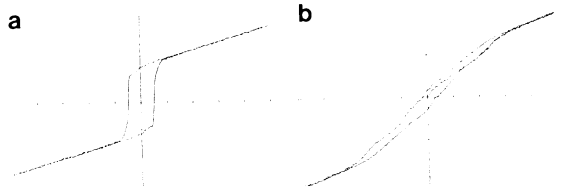

Figure 3. VSM curves for CoNiCr films deposited on [110] Cr single crystal measured along (a) [$\bar{1}$11] and (b) [$\bar{1}1\bar{1}$].

The magnetic domain structures on two different grain surfaces of the polycrystalline TEM specimens have also been studied. Long and relatively straight domain walls were found and they all lie along certain crystallographic directions through out the specimens. Figure 4 shows the magnetic domain structure of the CoNiCr film deposited on a (100) Cr surface. The contrast of the domain walls changes from over to underfocused conditions (Figures 4c and d). The domain walls are indicated by the black arrows. The angle between the two domain walls is measured to be approximately 78°. By correlating with the diffraction pattern, it was found that the convergent walls (bright in Figure 4c) lie along [$\bar{1}$101] and the divergent walls (dark) lie along [1$\bar{1}$01]. It is possible to deduce the direction of magnetization within the domain by considering the defocusing condition and the contrast of the wall. The magnetization direction within each domain is indicated by the white arrows and they were found to lie along the

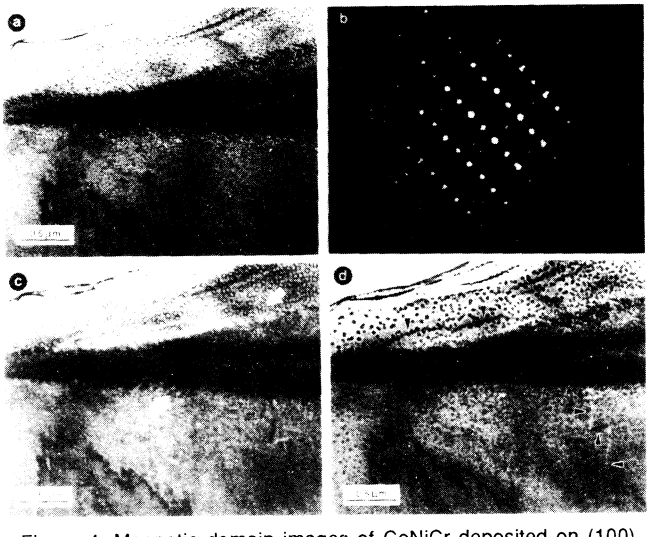

Figure 4. Magnetic domain images of CoNiCr deposited on (100) Cr surface. (a) focused, (b) corresponding SAD pattern, (c) overfocused and (d) underfocused. The domain walls are indicated by the black arrows (d). The direction of magnetization within the domain is along [0002] as indicated by the white arrows (c).

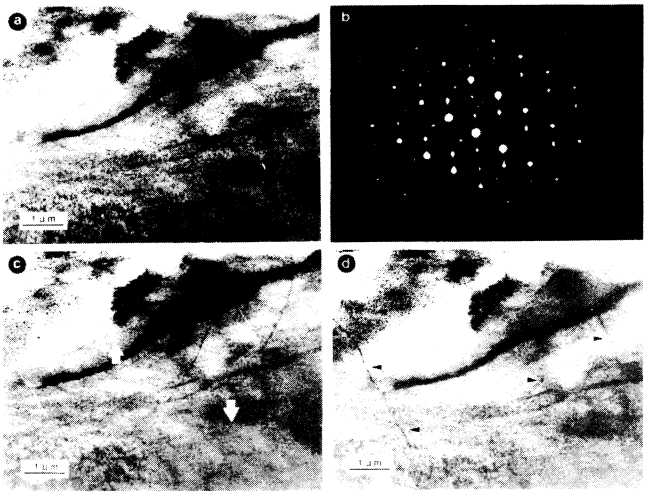

Figure 5. Magnetic domain images of CoNiCr deposited on (110) Cr surface. (a) focused, (b) corresponding SAD pattern, (c) underfocused and (d) overfocused. The domain walls are indicated by the black arrows (d). The direction of magnetization within the domain is along [0002] as indicated by the white arrows (c).

[0002] direction. Figure 5 shows similar images for the CoNiCr film deposited on a (110) surface. The angle between the domain walls is around 60° and the direction of magnetization was determined to be along the projection of the c-axis in the plane of the film. Thus, it is most likely along the c-axis. The divergent walls in Figure 5c were found to be nearly parallel to the $[\bar{1}101]$ and the convergent walls lie along the $[\bar{1}\bar{1}23]$ direction. Since the direction of best fit is along [0002] for the (001) surface, (0002)//(110), and along $[1\bar{1}1]$ for the (110) surface ,$(1\bar{1}1)//(11\bar{2}0)$, misfit accommodating defects should form along other directions. These defects could be domain wall pinning sites and thus the domain wall may lie along these directions of worst fit between the two surfaces. Figure 6 is a bright field image of the CoNiCr grains deposited on a (100) Cr surface. The picture shows the presence of two crystallographic variants and the grain size is the order of 200Å. Furthermore, there exists a high density of line defects inside each variant. These are the stacking faults which give rise to the streaking in the diffraction pattern. The dark field image taken from the $(1\bar{1}0)$ diffraction spot in the (110) surface is shown in Figure 7. There also exists two crystallographic variants with one of them being dominant. This may have caused the difference in the coercivity along $[\bar{1}1\bar{1}]$ and $[\bar{1}11]$ directions. Similarly, the film contains many line defects. These defects are perpendicular to the direction of the spot elongation in the diffraction patterns and hence they are stacking faults.

IV. Conclusion

CoNiCr films has been deposited on [100] and [110] Cr single crystal and polycrystalline Cr foils. An in plane crystallographic texture has been successfully obtained and TEM investigation shows the existence of crystallographic variants in the CoNiCr films. Lorentz images displayed relatively straight domain walls which lie along specific crystallographic axis and they have revealed that the magnetization lies along the c-axis within the domain. This texture gave rise to an anisotropy in the in-plane coercivity. The in-plane magnetic hysteresis loops are less square along the c-axis for either the (100) or (110) single crystal.

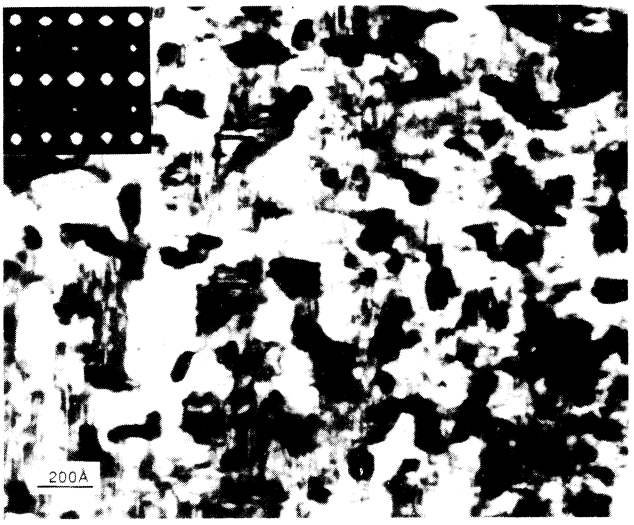

Figure 6. Bright field TEM image of CoNiCr/(100)Cr reveals the presence of two crystallographic variants. One of them is made up of the dark grains and the second one shows up as the bright background. One can also distinguish them by the stacking faults in the image.

Figure 7. Dark field TEM image of CoNiCr/(110)Cr taken with the $(1\bar{1}0)$ diffraction spot. There are two crystallographic variants present, represented by the white grains (arrow) and the background. They can also be distinguished by the trace of the stacking faults.

References

[1] J. P. Lazzari, I. Melnick, and D. Randet, IEEE Trans. Magn. **MAG-3**, 205 (1967).
[2] J. Daval and D.Randet, IEEE Trans. Mag. **MAG-6**, 768 (1970).
[3] K. Hono, B. Y. Wong, and D. E. Laughlin, J. Appl. Phys. **68**, 4734 (1990).
[4] S.L.Duan, J.O. Artman, B. Y. Wong and D.E.Laughlin, IEEE Trans. Mag. **MAG-26**, 1587 (1990).
[5] H. Hoffman, IEEE Trans. Mag. **MAG-9**, 17 (1973).
[6] H. Kronmüller, K-D. Durst and M. Sagawa, J. Magn. Magn. Mat. **74**, 291 (1987).